Physica D 51 (1991) 539–545
North-Holland

Electrodeposit tree patterns in linear cells: Experiment and computer models

R.D. Pochy, A. Garcia, R.D. Freimuth, V.M. Castillo and L. Lam
Nonlinear Physics Group, Department of Physics, San Jose State University, San Jose, CA 95192, USA

Fractal tree patterns are generated experimentally in electrodeposits of $CuSO_4$ in thin linear cells with relatively high voltages (15–30 V across two copper electrodes of separation 3.8 cm). The tree separations, tree widths and heights, and tree statistics are analysed. Tree pattern from two two-dimensional computer models, the three-directions biased random walk (BRW) model and the dielectric breakdown model (DBM) with probability cut-off, are produced. The BRW model compares very well with our experimental data. There is a minimum in the N_m versus m curve where N_m is the number of trees with mass m. For m small, $N_m \sim m^{-\tau}$ with $0 < \tau < 1$, in contrast to the DLA result that $1 < \tau < 2$. The fractal dimension of the tree D varies linearly with the fractal dimension of the walker D_w, which also differs from the DLA results of Matsushita et al. The DBM with cut-off gives trees with too much ramification compared to the experimental results, and fails to produce the sharp structure transition lines observed in previous electrodeposit experiments.

1. Introduction

It has been known for some time that different patterns can be generated in electrodeposits [1, 2] in thin, closed radial cells of $ZnSO_4$ solution by varying the voltage V and the concentration of the solutions C [3]. Similar and new patterns were obtained by our group [1, 4] in closed or open, radial or linear cells of $ZnSO_4$ and $CuSO_4$, respectively. In particular, (i) the very sensitive dependence of morphology on the cell thickness d was discovered. For example, three different morphologies (string, open ramified, and dendrite) were obtained in a single cell of varying thickness [1]. (ii) In linear cells dense linear morphologies (DLM) characterized by well-defined linear boundaries, the counterparts of the dense radial morphologies in radial cells [3], are discovered [4]. (iii) Compact fractal morphologies similar to viscous fingers in Hele–Shaw cells were found in both open and closed cells [1]. (iv) Depending on d two types of anode-sensitive sharp structure transition boundaries, induced by tip splitting or by fanning, were distinguished. (v) Power laws in time and space variables were obtained in the pattern growth.

In this paper, experimental results on electrodeposit tree patterns grown from $CuSO_4$ linear cells are presented. The voltage used is relatively high, 15–30 V across two parallel copper electrodes of 3.8 cm in separation. The cell thickness varied from 0.1–0.7 mm; the solution concentration is either 0.05 or 0.5 M. There is less ramification in these trees consisting of filaments, in comparison with those obtained by Matsushita et al. [5] in $ZnSO_4$ with 20 V between two electrodes of 10 cm apart. The latter is well described by the diffusion limited aggregate (DLA) model of Witten and Sander [6].

To simulate the trees produced by diffusion and electrical drift of the Cu ions in our experiments, the three-directions biased random walk model (BRW) [1] is used. Characteristics of the trees (average tree separation, tree heights and widths, and tree statistics) from this model agree very well with those from the experiments. The dependence of the tree fractal dimension, D, on the walker fractal dimension, D_w, is investigated.

For comparison the (unbiased) dielectric breakdown model (DBM) with probability cut-off, studied by Arian et al. [7] for a radial cell, is applied here for a linear cell. The trees from this generalized DBM, like the DLA, have too much ramification in comparison with the trees from our experiments. In spite of the existence of crossover from the usual DBM patterns to a spiky behavior the generalized DBM fails to produce the sharp structure transition (ST) lines observed in previous electrodeposit experiments [4].

2. Experimental results

The apparatus, experimental setup and procedure are the same as that described in ref. [4]. Two parallel copper electrodes with separation of 3.8 cm were used. The cell was placed horizontally. The ranges of V, C and d were chosen so that tree patterns were produced. The results shown in figs. 1–3 are the scans of the photographs taken when the majority of the trees were about $\frac{1}{4}$ to $\frac{1}{3}$ across the cell. The scan has 144 lines per inch. In some cases, such as those in fig. 3, sharp ST lines (not shown here) appeared in the further growth of the patterns (see fig. 7 of Ref. [4]).

As can be seen from figs. 1–3, all the three parameters V, C and d can influence the separation, thickness and branching of the trees. For example, the average tree separation, s, increases (decreases) with increasing d (V) when the other two parameters remain constant. Each picture in figs. 1–3 will be referred to as a forest.

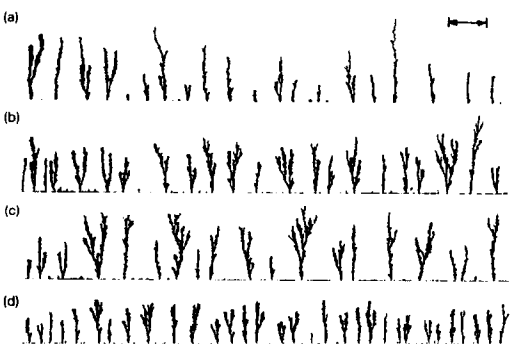

Fig. 1. Experimental trees formed by Cu deposits. Here and in figs. 2 and 3, scans from photographs are shown. $d = 0.7$ mm, $C = 0.5$ M. (a) $V = 15$ V, (b) $V = 20$ V, (c) $V = 25$ V, (d) $V = 30$ V. The indicated distance is 1 cm.

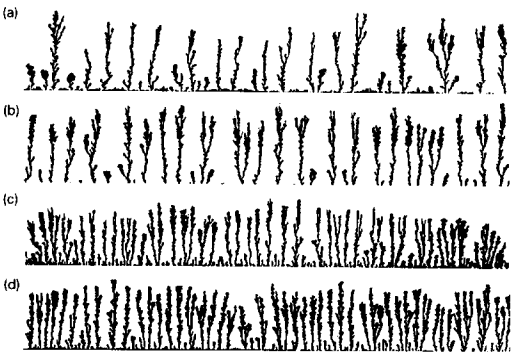

Fig. 2. Experimental trees formed by Cu deposits. $d = 0.6$ mm, $C = 0.05$ M; (a) $V = 15$ V, (b) $V = 20$ V, (c) $V = 25$ V, (d) $V = 30$ V.

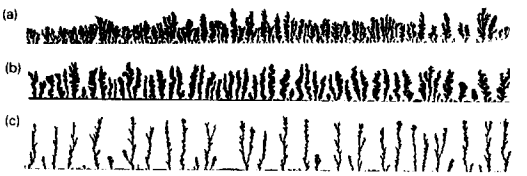

Fig. 3. Experimental trees formed by Cu deposits. $V = 20$ V, $C = 0.05$ M. (a) $d = 0.1$ mm, (b) $d = 0.4$ mm, (c) $d = 0.6$ mm.

The fractal dimension of each forest is calculated by both the box counting method and the correlation function method [8]. These two results are very close to each other. In fig. 4a the fractal dimension D obtained from the average from these two methods for each forest versus its mass density ρ is plotted. Here, $\rho \equiv N/A$ where N is the total number of dark pixels in the picture enclosed by a rectangular grid barely containing the forest, and A is the area of this grid. D varies from 1.26 to 1.80.

The height of a tree, h, is defined to be the distance between the farthest point in the tree from the base line, the cathode. For each forest the variation of h with m obeys a power law, $h \sim m^{\beta}$, where β varies slightly with each forest. Typical result is shown in fig. 5a. When averaged

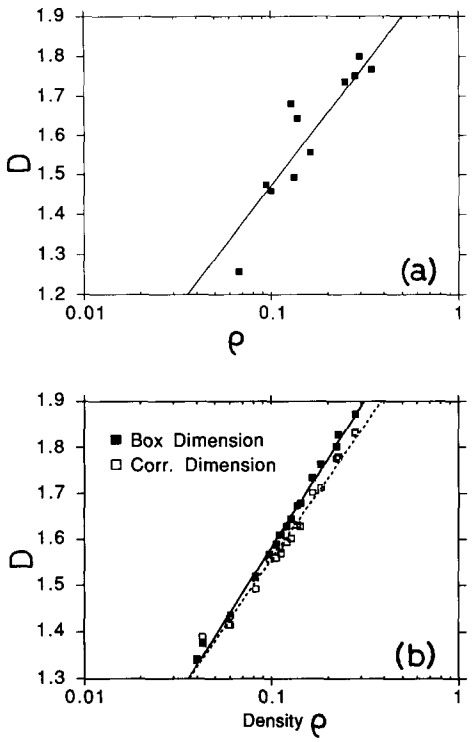

Fig. 4. Variation of fractal dimension D with mass density ρ. Each point comes from a forest. (a) From experimental data. D is the average of box and correlation dimensions. The straight line is the best fit given by $D = 2.08 + 0.61 \log \rho$. (b) Theoretical results from the BRW model. The straight line represents the best fit, $D = 2.22 + 0.64 \log \rho$, for the box dimensions; and $D = 2.14 + 0.58 \log \rho$, for the correlation dimensions.

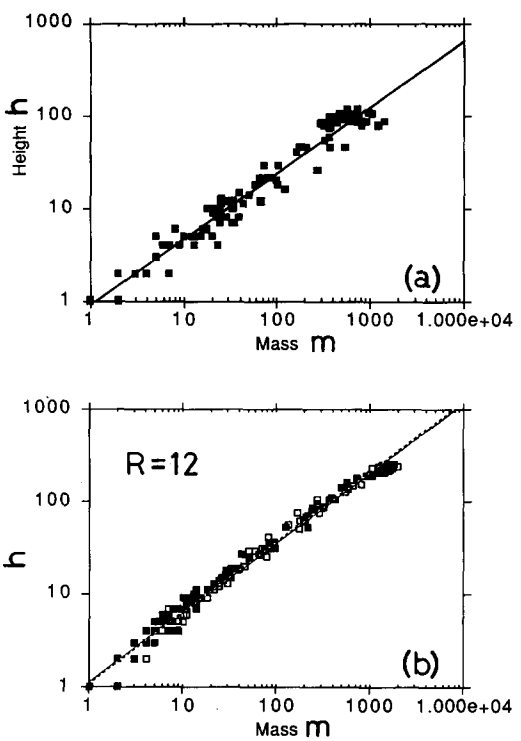

Fig. 5. Variation of tree height h with tree mass m. (a) Experimental result obtained from the third picture of fig. 2. (b) Theoretical result from the BRW model.

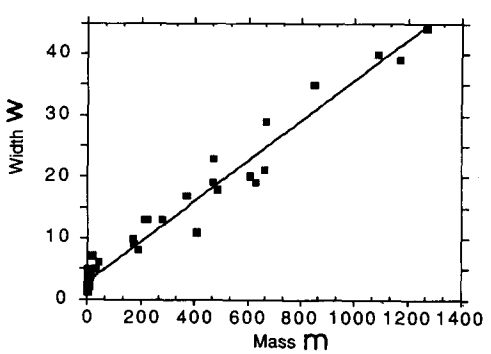

Fig. 6. Experimental tree width w versus tree mass m curve obtained from the middle picture of fig. 3. The straight line gives $w = w_0 + w_1 m$.

over the different forests, we found $\beta = 0.74 \pm 0.06$.

The width of a tree, w, is defined to be the largest span of the tree in the direction parallel to the base line. Approximately, for a given forest we found w varies linearly with m, i.e., $w = w_0 + w_1 m$. A typical result is depicted in fig. 6. As shown in fig. 7, for the four forests of fig. 1, both w_0 and w_1 vary linearly with V.

The average separation of trees in a forest, s, was found to decrease with ρ of that forest with a power law, $s \sim \rho^{-\gamma}$, as shown in fig. 8a where each point corresponds to a forest in figs. 1–3. Experimentally, $\gamma = 0.58$. For the three forests in fig. 3, s versus d is plotted in fig. 9.

The number of trees of mass m, N_m, as a function of m is shown in fig. 10a. For each forest there is a minimum in the N_m versus m curve at $m \approx 100$ before N_m drops rapidly at large m. For $m < 100$, one has approximately $N_m \sim m^{-\tau}$ with $0 < \tau < 1$. This is in contrast with the $ZnSO_4$

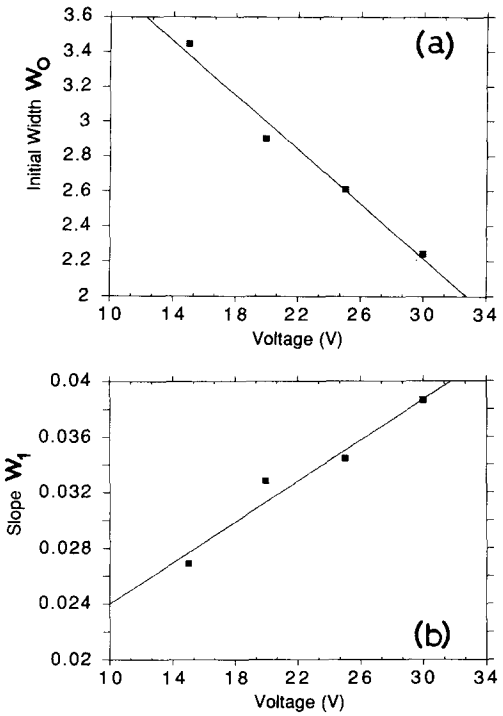

Fig. 7. Variation of w_0 and w_1 with voltage V from the four experimental pictures of fig. 1. (a) The best fit gives $w_0 = 4.555 - 0.078V$. (b) The best fit gives $w_1 = 0.017 + 0.000735V$. Here V is in volts.

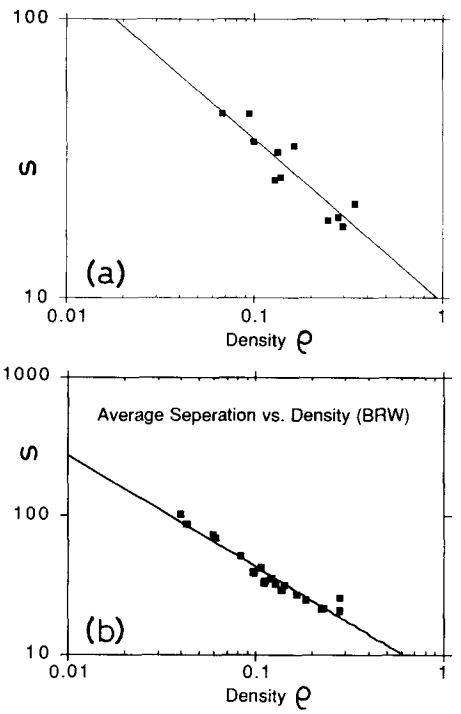

Fig. 8. Variation of average tree separation s with mass density ρ. (a) Experimental result. (b) Theoretical result from the BRW model.

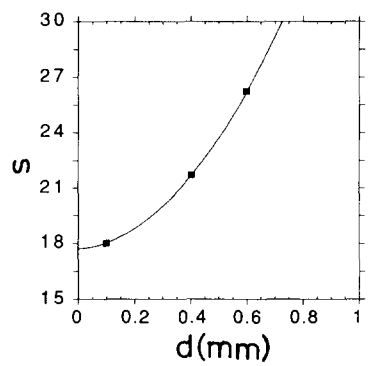

Fig. 9. Variation of average tree separation s with cell thickness d for the forests of fig. 3.

result of Matsushita et al. [5] where $\tau = 1.54$; in ref. [5] the initial electric field across the electrodes is 2 V/cm while ours is at least 4 V/cm. This decrease of τ is thus attributed to the high electric field applied.

3. The three-directions biased random walk model

To simulate the diffusion and drift of the ions at high electric field and to generate filaments of controllable widths, the three-directions biased random walk model (BRW) was introduced [1]. In this specific BRW model the walker in a square lattice is released randomly from the top and allowed to move sideward or downward, but not upward. This exclusion of the upward motion serves two purposes. First, the model has only one constant parameter, R, the ratio of the probabilities to move sideward to downward. Second, the computation is much faster. (The effect of the upward motion on the morphology produced is to increase slightly the ramification of the trees.) The simplest version is to allow the walker to

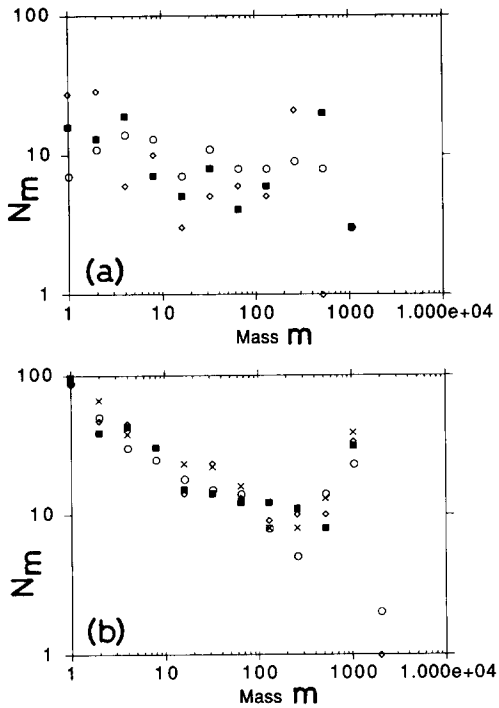

Fig. 10. Variation of N_m, number of trees of mass m, with tree mass m. (a) Experimental results. ■: from second picture of fig. 2, ○: from first picture of fig. 2, ◇: from third picture of fig. 3. (b) Theoretical results from the BRW model. ×: $R = 8$, ◇: $R = 10$, ■: $R = 12$, ○: $R = 15$.

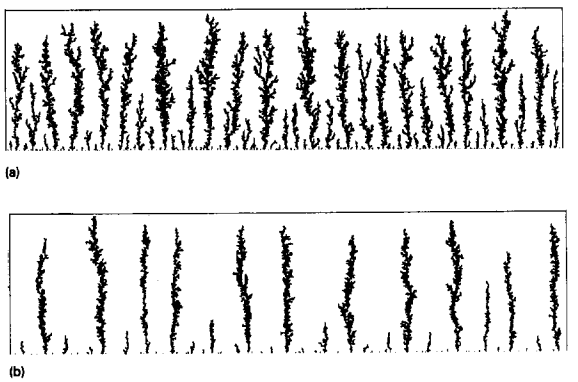

Fig. 11. Simulated forests from the BRW model. Grid size is 1024×256. (a) $R = 10$. (b) $R = 50$.

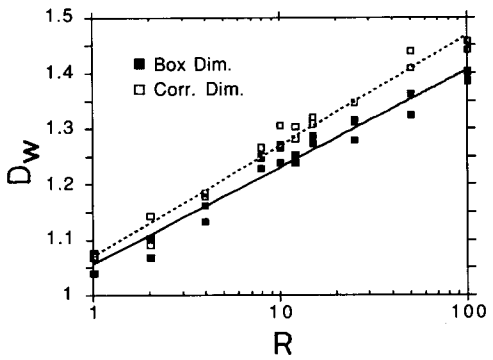

Fig. 12. Fractal dimension of the trajectory of the biased walker, D_w, versus R.

stick when it reaches the bottom base line or is on top or at the side of any part of the growing aggregate. Some of the simulations are shown in fig. 11 (see ref. [1] for more), which compare rather well with the experimental forests.

The fractal dimension of the trajectory of the walker, D_w, increases with R (fig. 12) according to $R = R_0 \exp(aD_w)$, with $R_0 = 2 \times 10^{-6}$ and $a = 13.16$ for the box dimension. One expects $D_w = 1$ for $R = 0$; $D_w = 2$ for $R \to \infty$; and so $1 < D_w < 2$.

The fractal dimension of the forest, D, changes with R according to $R = R_1 \exp(-bD)$; $R_1 = 1.36 \times 10^7$ and $b = 8.67$ for the box dimension (fig. 13a). The corresponding mass density ρ varies with R as $\rho = \rho_0 R^{-\delta}$; $\rho_0 = 0.31$ and $\delta = 0.42$. Figs. 13a and 13b may be combined to give fig. 4b, which agrees very well with the experiment data of fig. 4a.

Note that one has $D = -1.52 D_w + 3.47$, which differs from the theoretical expression, $D = (d^2 - 1 + D_w)/(d - 1 + D_w)$ with d = spatial dimension, for the radial cell obtained by Honda et al. [9].

Other typical results from the BRW model are given in figs. 5b, 8b, 10b and 14. The model gives $\beta = 0.75 \pm 0.03$ when averaged over R, in excellent agreement with the experiment. However, w increases with m in a power law (fig. 14a) while the experimental data (fig. 6) shows a linear law. The model also gives $\gamma = 0.80$ (fig. 8b), which is slightly larger than the experimental value of 0.58. Finally, the model gives the N_m versus m curves (fig. 10b) the shapes of which are in qualitative agreement with the experiments, and $0.31 < \tau < 0.46$. Note that, in contrast, simula-

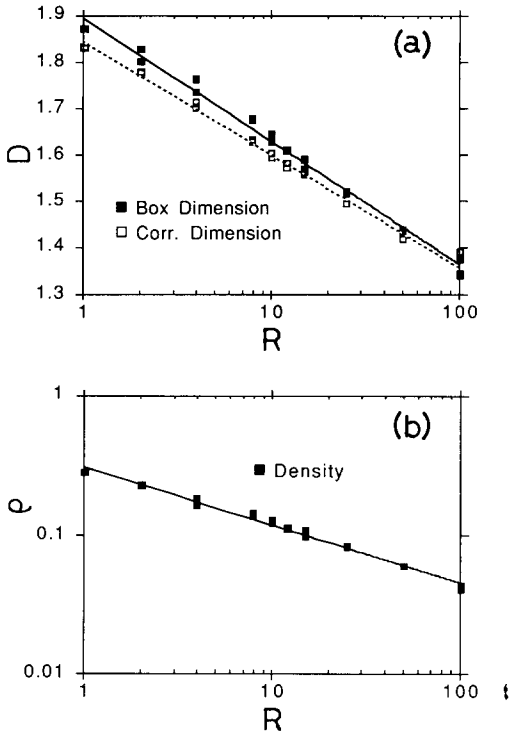

Fig. 13. Results from the BRW model. (a) Fractal dimension of the forest, D, versus R. (b) Mass density ρ versus R.

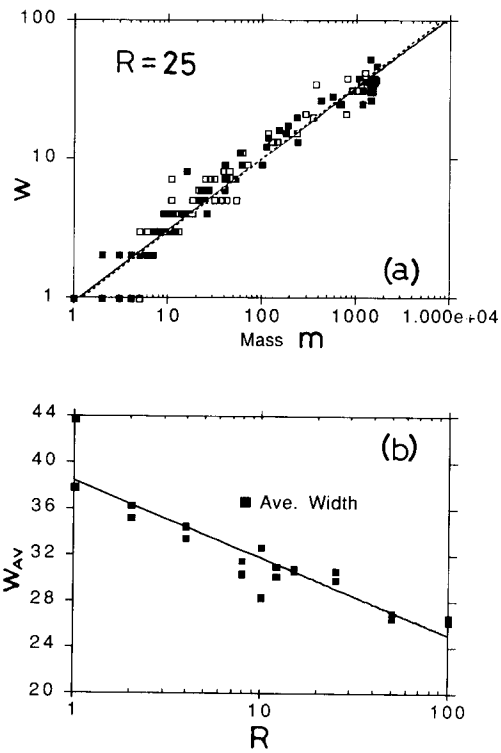

Fig. 14. Results from the BRW model. (a) Tree width w versus tree mass m. Two runs of data are shown. (b) Mean tree width w_{av} from each forest versus R.

tions and theory for purely diffusion-controlled deposition by Rácz and Vicsek [10] give $1 < \tau < 2$.

4. Dielectric breakdown model with probability cut-off

In the dielectric breakdown model (DBM), the field ϕ is solved from the Laplace equation $\nabla^2\phi = 0$. The probability of a perimeter site being occupied, $p_i \alpha (\nabla\phi)^\eta$. In the probability cut-off model, at every step only those sites with $p_i > p_c$ are kept where the cut-off probability p_c is a parameter. Each remaining site has now a new probability $p_i/(\Sigma_{p_i > p_c} p_i)$. This model with $\eta = 1$ has been applied to Arian et al. [7] in a 2D radial cell of square lattice to produce crossover behavior in the aggregates.

Our interest in this model is to apply it to a linear cell to see whether it can produce trees like those in our experiment, and whether it can produce the sharp ST lines [4]. Our square lattice has grid size 512×128. We have tried $\eta = \frac{1}{2}$, 1, $\frac{3}{2}$ and 2; $\alpha = 0$, 0.25, 0.5, 0.75 and 0.9 where $p_c = \alpha/512$. Some results are shown in fig. 15. As α increases, s decreases. The trees are found to have too much ramification compared to those in figs. 1–3. No sharp ST lines are found within the parameters used here. The fractal dimensions of the forests are shown in fig. 16; the slope of the straight line (D versus $\log \rho$) is 0.50 which is slightly less than 0.64, the value for the BRW model (fig. 4b).

5. Discussions

The three-directions BRW model does give trees and forests resembling the experimental results. Except for some discrepancies in the tree

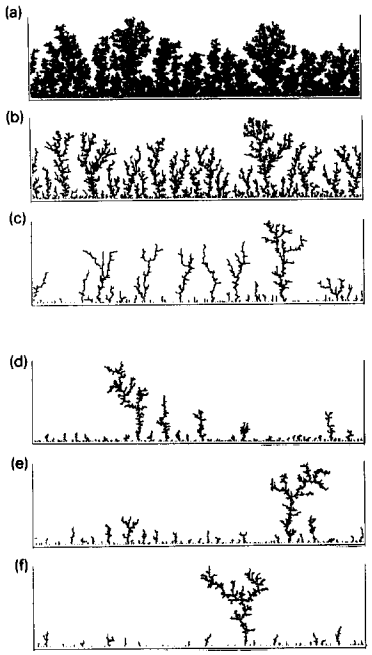

Fig. 15. Forests from the DBM with cut-off. $\eta = \frac{1}{2}$ in (a)–(c); $\eta = \frac{3}{2}$ in (d)–(f). $\alpha = 0$ in (a), (d); $\alpha = 0.5$ in (b), (e); $\alpha = 0.9$ in (c), (f).

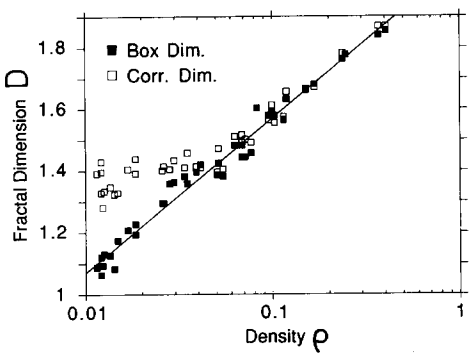

Fig. 16. Fractal dimension D versus mass density ρ from the DRM with cut-off.

width w there are many quantitative agreements between the model and the experiments. Perhaps the rms tree height and width (instead of the absolute tree height and width used here) will give better description and better agreement. Results from the BRW model differ from the DLA-type model in several important aspects. For example, in the former $0 < \tau < 1$ and D is linear in D_w.

Realistically, the "bias" in the BRW model is related to the electric field which should be determined by the instantaneous configurations of the trees, and is not constant as assumed in our model. That is, the "bias" should be built into the DBM model. Whether our results are sensitive to this modification and to noise remains to be explored.

To produce the experimental trees it seems some bias of the walker is essential in the computer model. It will be of interest to incorporate bias into the DBM with cut-off in the future.

Acknowledgement

This work is supported by a grant from Research Corporation.

References

[1] L. Lam, R.D. Pochy and V.M. Castillo, in: Nonlinear Structures in Physical Systems, eds. L. Lam and H.C. Morris (Springer, New York, 1990).
[2] L.M. Sander, in: The Physics of Structure Formation, eds. W. Guttinger and G. Dangelmayr (Springer, New York, 1987).
[3] Y. Sawada, A. Dougherty and J.P. Gollub, Phys. Rev. Lett. 56 (1986) 1260;
D. Grier, E. Ben-Jacob, R. Clarke and L.M. Sander, Phys. Rev. Lett. 56 (1986) 1264.
[4] M.A. Guzman, R.D. Freimuth, P.U. Pendse, M.C. Veinott and L. Lam, in: Nonlinear Structures in Physical Systems, eds. L. Lam and H.C. Morris (Springer, New York, 1990).
[5] M. Matsushita, Y. Hayakawa and Y. Sawada, Phys. Rev. A 32 (1985) 3814.
[6] T.A. Witten and L.M. Sander, Phys. Rev. Lett. 47 (1981) 1400.
[7] E. Arian, P. Alstrom, A. Aharony and H.E. Stanley, Phys. Rev. Lett. 63 (1989) 2005.
[8] T.S. Parker and L.O. Chua, Practical Numerical Algorithms for Chaotic Systems (Springer, New York, 1989).
[9] K. Honda, H. Toyoki and M. Matsushita, J. Phys. Soc. Japan 55 (1986) 707.
[10] Z. Rácz and T. Vicsek, Phys. Rev. Lett. 51 (1983) 2382.